

Combining pair-density functional theory and variational two-electron reduced-density matrix methods

Mohammad Mostafanejad¹ and A. Eugene DePrince III¹

¹ *Department of Chemistry and Biochemistry, Florida State University, Tallahassee, FL 32306-4390*

Complete active space self-consistent field (CASSCF) computations can be realized at polynomial cost via the variational optimization of the active-space two-electron reduced-density matrix (2-RDM). Like conventional approaches to CASSCF, variational 2-RDM (v2RDM)-driven CASSCF captures nondynamical electron correlation in the active space, but it lacks a description of the remaining dynamical correlation effects. Such effects can be modeled through a combination of v2RDM-CASSCF and on-top pair-density functional theory (PDFT). The resulting v2RDM-CASSCF-PDFT approach provides a computationally inexpensive framework for describing both static and dynamical correlation effects in multiconfigurational and strongly correlated systems. On-top pair-density functionals can be derived from familiar Kohn-Sham exchange-correlation (XC) density functionals through the translation of the v2RDM-CASSCF reference densities [Li Manni *et al.*, *J. Chem. Theory Comput.* **10**, 3669-3680 (2014)]. Translated and fully-translated on-top PDFT versions of several common XC functionals are applied to the potential energy curves of N₂, H₂O, and CN⁻, as well as to the singlet/triplet energy splittings in the linear polyacene series. Using v2RDM-CASSCF-PDFT and the translated PBE functional, the singlet/triplet energy splitting of an infinitely-long acene molecule is estimated to be 4.87 kcal mol⁻¹.

I. INTRODUCTION

The accurate and computationally affordable description of the electronic structure of many-body systems remains a major challenge within the quantum chemistry and molecular physics communities.[1–3] Specifically, the realization of general approaches that account for both dynamical and nondynamical correlation effects in multiconfigurational [4] or strongly-correlated systems is particularly difficult. The main issue is that many approaches designed to deal with multireference (MR) problems are not particularly efficient for capturing dynamical correlation effects. A similar statement can be made regarding the ability of methods designed to model dynamical correlation to capture MR effects.

One can broadly classify approaches to the electron correlation problem as either falling within wave function theory (WFT), in which the many-electron wave function is obviously the central quantity, [5–7] or density-based theories, which include both density functional theory (DFT) [8–12] and reduced-density matrix (RDM)-based approaches. [13–17] In principle, WFT is preferable, as it allows for systematic improvement in the calculated energies and properties of the system.[18] In practice, however, the computational complexity of post-Hartree-Fock wave-function-based methods, specifically MR approaches, limits their application to small systems.[19] The wide-ranging success of DFT, on the other hand, stems from its ability to provide a reasonable description of electron correlation at significantly lower costs. Nonetheless, DFT often fails for MR systems, and it does not offer a systematic approach for improving its accuracy. [8–12]

Within WFT, one of the most familiar approaches to the MR problem is the complete active space self-consistent field (CASSCF) method [20–23]. In CASSCF,

the molecular orbitals are partitioned into inactive (doubly occupied), active (partially occupied), and external (empty) orbitals, and the active space is chosen with some knowledge as to which orbitals are important for the chemical problem at hand. In the canonical form of CASSCF, the active-space electronic structure is described by a full configuration interaction (CI) wave function, and it is assumed that all nondynamical correlation effects are captured by this procedure. Dynamical correlation effects can then be incorporated through a variety of approaches, including perturbation theory (using, for example, complete active space second-order perturbation theory (CASPT2) [24, 25]). CASPT2 requires knowledge of the four-electron reduced-density matrix (4-RDM), or some approximation to it, which can become problematic as the size of the active space increases. Accordingly, several approaches have been proposed that eliminate the manipulation of the 4-RDM, including the anti-Hermitian contracted Schrödinger equation (ACSE) [26–28] and the driven similarity renormalization group (DSRG) [29]. Both of these approaches require knowledge of the three-electron reduced-density matrix (3-RDM).

A long sought-after alternative to the methods described above involves the combination of the MR approach to the static correlation problem with a DFT-based description of dynamical correlation. Since the advent of the MR+DFT framework, [30, 31] a substantial amount of effort has been devoted to increasing the accuracy and efficiency of this approach. [32–50] There are several issues that one must carefully consider when developing a MR+DFT scheme, including (i) the symmetry dilemma that plagues Kohn-Sham (KS)-DFT in general, (ii) the double counting of electron correlation within the active space, and (iii) the steep computational scaling of many commonly used MR methods. The framework of the multiconfiguration-pair-density func-

tional theory (MC-PDFT) [51, 52] addresses the first two issues while leaving open the question of the cost of the evaluation of the underlying MR wave function. The success of the original formulation of MC-PDFT[52] notwithstanding, Garza *et al.*[32] rightly note that, if the MR component is determined using an approach such as CASSCF, its utility is potentially limited by the exponential complexity of the CI-based active-space wave function. Hence, those authors propose that the static correlation within MC-PDFT be described by the pair coupled-cluster doubles (pCCD) method,[53, 54] the scaling of which increases as only $\mathcal{O}(k^4)$ or $\mathcal{O}(k^5)$, where k is the size of the one-electron basis set; the specific scaling is determined by the treatment of the orbital transformation step. More recently, the MC-PDFT scheme has also been employed in conjunction with other active-space-based methods that scale more favorably than CASSCF, including the density matrix renormalization group (DMRG)[55] and the generalized active-space self-consistent field (GASSCF)[56].

Here, we offer an alternative strategy to overcome the problematic scaling of CI-based CASSCF within the MC-PDFT framework. We elect to maintain the CASSCF-based description of the static correlation problem utilized in the original formulation of the approach,[52] but we represent the electronic structure of the active space with the two-electron reduced-density matrix (2-RDM), as opposed to the CI wave function. The computational complexity of variational 2-RDM-driven CASSCF (v2RDM-CASSCF) [57, 58] increases only polynomially with the size of the active space, thereby facilitating v2RDM-based MC-PDFT computations (denoted v2RDM-CASSCF-PDFT) on active spaces as large as 50 electrons in 50 orbitals.

This paper is organized as follows. Section II provides an overview of v2RDM-CASSCF-PDFT, including brief discussions of the theory underlying the v2RDM-CASSCF and MC-PDFT schemes. The computational details of the work are then given in Sec. III. In Sec. IV, we provide evidence of the correctness of our v2RDM-CASSCF-PDFT implementation by comparing singlet/triplet energy splittings for a set of main-group divalent radicals to those obtained from conventional, CI-CASSCF-driven MC-PDFT.[59] We then apply v2RDM-CASSCF-PDFT to the potential energy curves (PECs) of N_2 , H_2O , and CN^- , as well as to the singlet/triplet energy gaps of the linear polyacene series. Some concluding remarks can be found in Sec. V.

II. THEORY

Throughout this work, we adopt the conventional notation employed within MR methods for labeling molecular orbitals (MOs, $\{\psi\}$): the indices i, j, k , and l represent inactive orbitals; t, u, v , and w indicate active orbitals; a, b, c , and d denote external orbitals; and p, q, r , and s represent general orbitals.

Let Ψ be an N -electron wave function in Fock space. One- and two- particle excitation operators can be expressed as [5]

$$\hat{E}_q^p = \hat{a}_{p\sigma}^\dagger \hat{a}_{q\sigma} \quad (1a)$$

$$\hat{e}_{qs}^{pr} = \hat{E}_q^p \hat{E}_s^r - \delta_r^q \hat{E}_s^p = \hat{a}_{p\sigma}^\dagger \hat{a}_{r\tau}^\dagger \hat{a}_{s\tau} \hat{a}_{q\sigma} \quad (1b)$$

where \hat{a}^\dagger and \hat{a} represent second-quantized creation and annihilation operators, respectively, and the Greek labels run over α and β spins. Einstein's summation convention is implied throughout. The non-relativistic Born-Oppenheimer (BO) electronic Hamiltonian is

$$\hat{\mathcal{H}} = h_q^p \hat{E}_q^p + \frac{1}{2} \nu_{rs}^{pq} \hat{e}_{rs}^{pq} \quad (2)$$

where $h_q^p = \langle \psi_p | \hat{h} | \psi_q \rangle$ is the sum of the electron kinetic energy and electron-nucleus potential energy integrals, and $\nu_{rs}^{pq} = \langle \psi_p \psi_q | \psi_r \psi_s \rangle$ represents the two-electron repulsion integral tensor. Because the electronic Hamiltonian includes up to only pair-wise interactions, the ground-state energy of a many-electron system can be expressed as an exact linear functional of the 2-RDM and the one-electron reduced-density matrix (1-RDM) [60–62]

$$E = {}^1D_q^p h_q^p + \frac{1}{2} {}^2D_{rs}^{pq} \nu_{rs}^{pq}. \quad (3)$$

Here, the 1-RDM and the 2-RDM are represented in their spin-free forms, defined as

$${}^1D_q^p = {}^1D_{q\sigma}^{p\sigma} = \langle \Psi | \hat{E}_q^p | \Psi \rangle \quad (4)$$

and

$${}^2D_{rs}^{pq} = {}^2D_{r\sigma s\tau}^{p\sigma q\tau} = \langle \Psi | \hat{e}_{rs}^{pq} | \Psi \rangle. \quad (5)$$

Summation over the spin labels is implied.

A. v2RDM-driven CASSCF

The CASSCF non-relativistic BO electronic Hamiltonian is

$$\hat{\mathcal{H}}_{\text{CASSCF}} = (h_u^t + 2\nu_{ui}^{ti} - \nu_{ii}^{tu}) \hat{E}_u^t + \frac{1}{2} \nu_{uv}^{tu} \hat{e}_{uv}^{tu}, \quad (6)$$

and the CASSCF active-space electronic energy is expressible in terms of the active-space 1- and 2-RDMs

$$E_{\text{CASSCF}} = (h_u^t + 2\nu_{ui}^{ti} - \nu_{ii}^{tu}) {}^1D_u^t + \frac{1}{2} \nu_{uv}^{tu} {}^2D_{uv}^{tu}. \quad (7)$$

The central idea of v2RDM-CASSCF is that the spin blocks of the active-space RDMs can be determined directly by minimizing the energy with respect to variations in their elements (and to variations in the orbital parameters).[57, 58] Because not every 2-RDM can be derived from an N -electron wave function, this procedure can lead to unphysically low energies:[13] a

physically meaningful 2-RDM should fulfill certain N -representability conditions. These conditions are most easily expressed in terms of the individual spin blocks that contribute to the spin-free 2-RDM. Specifically, each spin block of the 2-RDM should (i) be Hermitian, (ii) be antisymmetric with respect to the permutation of particle labels, (iii) conserve the number of pairs of particles (have a fixed trace), and (iv) contract to the appropriate spin block(s) of the 1-RDM. Constraints on the expectation value of \hat{S}^2 can also be applied.[63]

In addition to these trivial constraints on the 2-RDM, all spin blocks of all RDMs should be positive semidefinite. Such positivity conditions applied to the spin blocks of the 2-RDM, the two-hole RDM, and the particle-hole RDM constitute the two-body (PQG) constraints of Garrod and Percus.[64] Additional positivity conditions can be applied to higher-order RDMs. In this work, we consider the PQG constraints as well as the T2 partial three-particle condition.[65, 66] The spin blocks of each of these RDMs are interrelated through linear mappings implied by the anticommutation properties of the creation and annihilation operators that define them. The v2RDM-CASSCF procedure thus involves a large-scale semidefinite optimization that we carry out using a boundary-point algorithm [67–69], the specific details of which can be found in Ref. 58.

B. Multi-configuration Pair-Density Functional Theory

One of the main pitfalls of the MR+DFT scheme is the double counting of electron correlation within the active space. The most expedient solution is to employ a small active space or modified functionals;[30, 31, 33] such strategies may not always lead to satisfactory results, though. A seemingly robust solution[52] partitions the interelectronic Coulomb contribution to the energy into a classical Coulomb component (obtained from an MR method) and all other exchange and pure two-electron contributions (described by DFT). Because the two-electron correlations are modeled entirely within the framework of DFT, double counting of such contributions to the energy is automatically avoided. However, this strategy offers no such guarantee regarding the double counting of *kinetic* correlation.

A second complication in MR+DFT is related to the “symmetry dilemma” [70] of standard KS-DFT. One manifestation of this issue within MR+DFT is the incompatibility of standard XC functionals with MR spin densities for low-spin (i.e. $|M_S| < S$) states. Fortunately, this difficulty is easily overcome by replacing the usual independent variables that enter KS-DFT XC functionals, the total density, $\rho(\mathbf{r}) = \rho_\alpha(\mathbf{r}) + \rho_\beta(\mathbf{r})$, and the spin magnetization, $m(\mathbf{r}) = \rho_\alpha(\mathbf{r}) - \rho_\beta(\mathbf{r})$, with the total density and the on-top pair-density (OTPD), $\Pi(\mathbf{r})$.[35, 70, 71]

Both double counting and the symmetry dilemma are addressed through the framework of MC-PDFT,[52] in

which the active-space electronic energy is defined as

$$E_{\text{MC-PDFT}} = (h_u^t + 2\nu_{ui}^{ti})^1 D_u^t + \frac{1}{2} \nu_{uv}^{tv} {}^1 D_u^t {}^1 D_w^v + E_{\text{OTPD}}[\rho(\mathbf{r}), \Pi(\mathbf{r}), |\nabla\rho(\mathbf{r})|, |\nabla\Pi(\mathbf{r})|]. \quad (8)$$

Here, the two-electron term from Eq. 7 has been replaced by a classical Coulombic term, and the remaining exchange and correlation effects are folded into a functional of the OTPD. The total electronic density and its gradient are defined by the 1-RDM as

$$\rho(\mathbf{r}) = {}^1 D_q^p \psi_p^*(\mathbf{r}) \psi_q(\mathbf{r}), \quad (9)$$

and

$$\nabla\rho(\mathbf{r}) = {}^1 D_q^p [\nabla\psi_p^*(\mathbf{r})\psi_q(\mathbf{r}) + \psi_p^*(\mathbf{r})\nabla\psi_q(\mathbf{r})], \quad (10)$$

respectively. The OTPD and its gradient can similarly be defined in terms of the 2-RDM as

$$\Pi(\mathbf{r}) = {}^2 D_{rs}^{pq} \psi_p^*(\mathbf{r}) \psi_q^*(\mathbf{r}) \psi_r(\mathbf{r}) \psi_s(\mathbf{r}), \quad (11)$$

and

$$\begin{aligned} \nabla\Pi(\mathbf{r}) = {}^2 D_{rs}^{pq} [& \nabla\psi_p^*(\mathbf{r})\psi_q^*(\mathbf{r})\psi_r(\mathbf{r})\psi_s(\mathbf{r}) \\ & + \psi_p^*(\mathbf{r})\nabla\psi_q^*(\mathbf{r})\psi_r(\mathbf{r})\psi_s(\mathbf{r}) \\ & + \psi_p^*(\mathbf{r})\psi_q^*(\mathbf{r})\nabla\psi_r(\mathbf{r})\psi_s(\mathbf{r}) \\ & + \psi_p^*(\mathbf{r})\psi_q^*(\mathbf{r})\psi_r(\mathbf{r})\nabla\psi_s(\mathbf{r})], \quad (12) \end{aligned}$$

respectively. Here, the 1- and 2-RDMs are obtained from an MR computation.

Armed with a potentially robust framework for MR+DFT, we must identify a suitable OTPD functional for use within MC-PDFT. The simplest class of functionals can be derived from existing approximate XC functionals employed within KS-DFT by first recognizing that, for a density derived from a single Slater determinant, the spin magnetization can be expressed exactly in terms of the OTPD and the total density.[35, 71] More specifically, the spin polarization factor, $\zeta(\mathbf{r}) = m(\mathbf{r})/\rho(\mathbf{r})$, can be expressed as

$$\zeta(\mathbf{r}) = \sqrt{1 - R(\mathbf{r})}, \quad (13)$$

where

$$R(\mathbf{r}) = \frac{4 \Pi(\mathbf{r})}{\rho^2(\mathbf{r})}. \quad (14)$$

The basic assumption underlying the “translated” (t) OTPD functionals proposed in Ref. 52 is that the spin polarization factor can be similarly defined for a density and OTPD obtained from a MR method, as

$$\zeta_t(\mathbf{r}) = \begin{cases} \sqrt{1 - R(\mathbf{r})} & R(\mathbf{r}) \leq 1 \\ 0 & R(\mathbf{r}) > 1 \end{cases} \quad (15)$$

where the second case accounts for the fact that the argument of the square root can become negative for $\rho(\mathbf{r})$

and $\Pi(\mathbf{r})$ that are not derived from a single-configuration wave function. The translated OTPD functional is then defined as

$$E_{\text{OTPD}}[\rho(\mathbf{r}), \Pi(\mathbf{r}), |\nabla\rho(\mathbf{r})|] \equiv E_{\text{XC}}[\tilde{\rho}_\alpha(\mathbf{r}), \tilde{\rho}_\beta(\mathbf{r}), |\nabla\tilde{\rho}_\alpha(\mathbf{r})|, |\nabla\tilde{\rho}_\beta(\mathbf{r})|], \quad (16)$$

where the tilde refers to translated densities and their gradients, given by [51, 52]

$$\tilde{\rho}_\sigma(\mathbf{r}) = \frac{\rho(\mathbf{r})}{2} (1 + c_\sigma \zeta_t(\mathbf{r})), \quad (17)$$

and

$$\nabla\tilde{\rho}_\sigma(\mathbf{r}) = \frac{\nabla\rho(\mathbf{r})}{2} (1 + c_\sigma \zeta_t(\mathbf{r})), \quad (18)$$

respectively. Here, $c_\sigma = 1$ (-1) when $\sigma = \alpha$ (β).

It is important to note that, in deriving the translated OTPD functional expression in Eq. 16, no dependence on $\nabla\Pi(\mathbf{r})$ is assumed. A scheme in which the OTPD functional depends explicitly upon $\nabla\Pi(\mathbf{r})$ has also been proposed.[72] The corresponding “fully-translated” (ft) functionals are defined as

$$E_{\text{OTPD}}[\rho(\mathbf{r}), \Pi(\mathbf{r}), |\nabla\rho(\mathbf{r})|, |\nabla\Pi(\mathbf{r})|] \equiv E_{\text{XC}}[\tilde{\rho}_\alpha(\mathbf{r}), \tilde{\rho}_\beta(\mathbf{r}), |\nabla\tilde{\rho}_\alpha(\mathbf{r})|, |\nabla\tilde{\rho}_\beta(\mathbf{r})|] \quad (19)$$

Expressions for the fully-translated spin densities and their respective gradients, taken from Ref. 73, are provided in the Appendix.

III. COMPUTATIONAL DETAILS

The 1- and 2-RDMs entering Eqs. 9-12 are obtained from v2RDM-CASSCF computations using the v2RDM-CASSCF plugin [74] to the Psi4 electronic structure package. [75] The v2RDM-CASSCF procedure is state specific; the orbitals are optimized for the ground state of a given spin symmetry. For v2RDM-CASSCF-PDFT, we have implemented translated and fully-translated versions of the Slater and Vosko-Wilk-Nusair random-phase approximation expression III (SVWN3), [76–78] Perdew-Burke-Ernzerhof (PBE) [79] and Becke and Lee-Yang-Parr (BLYP) [80, 81] XC functionals. The XC energy, along with the one-electron and classical Coulomb contributions to the MC-PDFT energy (Eq. 8) are evaluated using a new plugin to Psi4.[82]

The results of v2RDM-CASSCF-PDFT computations of the PECs for N_2 , H_2O , and CN^- are compared to those from reference computations performed using CASPT2, as implemented in the OPEN-MOLCAS electronic structure package. [83] The standard imaginary shift [84] of $0.20 E_h$ and OPEN-MOLCAS’s default value of $0.25 E_h$ for ionization potential electron affinity (IPEA) [85] were applied in all CASPT2 computations. All CASPT2 computations employed a full-valence CI-driven CASSCF reference.

All v2RDM-CASSCF-PDFT computations employ the density-fitting approximation to the electron repulsion integrals.[86, 87] The N_2 , H_2O , and CN^- PECs were computed using full-valence v2RDM-CASSCF, the cc-pVTZ basis set,[88] and the corresponding JK-type auxiliary basis set.[89] The details of the full-valence active spaces can be found in the Supporting Information. Singlet/triplet energy gaps for the linear polyacene series were computed within the cc-pVTZ basis with the corresponding JK-type auxiliary basis set. Here, the v2RDM-CASSCF computations employ a $(4k+2, 4k+2)$ active space ($2k+1$ π bonding orbitals and $2k+1$ antibonding π^* orbitals), where k represents the number of fused six-membered rings in the polyacene molecule. Equilibrium geometries for the singlet and triplet states of the polyacene series were determined at the v2RDM-CASSCF/cc-pVDZ level of theory using a development version of the Q-Chem 5.1 electronic structure package[90] and the analytic gradient implementation described in Ref. 91.

IV. RESULTS AND DISCUSSION

As evidence of the correctness of our implementation of v2RDM-CASSCF-PDFT, we compare singlet/triplet energy splittings evaluated using this approach to those obtained from conventional, CI-CASSCF-driven MC-PDFT. The test set was comprised of the main-group divalent radicals considered in Ref. 59. Equilibrium geometries for these molecules, as well as MC-PDFT and experimentally-derived singlet/triplet energy splittings were taken from that work and the references therein. The present v2RDM-CASSCF-PDFT computations employed a full-valence active space, the aug-cc-pVQZ basis set,[92] and the corresponding JK-type auxiliary basis set; the active space details can be found in the Supporting Information. When enforcing the PQG and T2 N -representability conditions, v2RDM-CASSCF-PDFT singlet/triplet gaps are in excellent agreement with those from MC-PDFT (when using the same primary basis and active space). For example, the mean absolute errors in the v2RDM-CASSCF-PDFT gaps, relative to those from experiment, are 5.4, 7.1, 9.7, and 12.4 kcal mol⁻¹ when using the translated PBE, translated BLYP, fully-translated PBE, and fully-translated BLYP functionals, respectively. The mean errors from MC-PDFT are 5.5, 7.2, 9.6, and 12.3 kcal mol⁻¹ when using the same functionals. The agreement between v2RDM-CASSCF-PDFT and MC-PDFT is slightly worse when v2RDM-CASSCF-PDFT employs RDMs that satisfy only the PQG N -representability conditions; in this case, when using the same functionals, v2RDM-CASSCF-PDFT displays mean errors of 4.9, 6.3, 8.5, and 10.9 kcal mol⁻¹. Oddly enough, the gaps derived from computations involving the PQG conditions are slightly more accurate than those from v2RDM-CASSCF-PDFT with the PQG+T2 conditions or from MC-PDFT. The v2RDM-

CASSCF-PDFT singlet/triplet energy splittings are tabulated alongside those from (v2RDM-)CASSCF, MC-PDFT, and CASPT2 in the Supporting Information.

A. Potential Energy Curves

Figure 1(a) provides dissociation curves for molecular nitrogen computed at the v2RDM-CASSCF, CASPT2, and v2RDM-CASSCF-PDFT levels of theory. The 2-RDMs in the v2RDM-CASSCF computations satisfied the PQG N -representability conditions. The v2RDM-CASSCF-PDFT computations employed the translated variants of the SVWN3, PBE, and BLYP functionals (denoted tSVWN3, tPBE, and tBLYP, respectively). Figure 1(b) illustrates the dissociation limit for each method, where each curve is shifted such that the energy at 3.0 Å is zero E_h . The overall shape of the CASPT2 PEC is reasonably reproduced by both the v2RDM-CASSCF and v2RDM-CASSCF-PDFT methods, but we note that the dissociation limits of CASPT2 (with an IPEA shift of 0.25 E_h) and tBLYP show an unphysical hump at 3.7 and 3.5 Å, respectively. Table I provides the non-parallelity errors (NPEs) for the PECs computed using each method. The NPE is defined as the difference between the maximum and minimum errors in each curve, using CASPT2 as a reference. For N_2 , the NPEs in the v2RDM-CASSCF, tSVWN3, tPBE, and tBLYP PECs are 35.5, 91.8, 17.7, and 20.9 mE_h , respectively; for comparison, the NPE for CI-based CASSCF (not illustrated in Fig. 1) is 30.1 mE_h . With the exception of v2RDM-CASSCF and tBLYP, the maximum error contributing to the NPE occurs at 5.0 Å, after CASPT2 begins to fail. Table I also provides NPEs computed when the v2RDM-CASSCF and v2RDM-CASSCF-PDFT computations were carried out using RDMs that satisfy the PQG+T2 N -representability conditions (the corresponding dissociation curves can be found in the Supporting Information). The NPE is 29.5 mE_h for v2RDM-CASSCF, which is in much better agreement with that from CI-based CASSCF. The NPEs for v2RDM-CASSCF-PDFT appear to be less sensitive to the N -representability of the RDMs; the largest change we observe is for tBLYP, where the NPE is reduced by 2.7 mE_h .

The remaining two panels in Fig. 1 illustrate the same PECs, but the v2RDM-CASSCF-PDFT computations employed the fully-translated variants of SVWN3, PBE, and BLYP functionals (denoted ftSVWN3, ftPBE, and ftBLYP, respectively). In terms of absolute energies, full translation universally lowers the energy obtained from v2RDM-CASSCF-PDFT using all functionals, relative to the case in which regular translation was employed. The computed NPEs are considerably worse, increasing by as much as 12.0 and 12.1 mE_h in the cases of ftPBE and ftBLYP, respectively. Notably, full translation improves the qualitative description of the dissociation limit in the case of ftBLYP. Again, as can be seen in Table I, the NPEs for fully-translated functionals are quite insensi-

tive to the N -representability of the reference RDMs.

Figure 2 illustrates PECs corresponding to the symmetric double dissociation of H_2O , with a fixed H–O–H angle of 104.5°, computed using the same levels of theory discussed above. Similar conclusions can be drawn in this case, regarding the qualitative agreement of the shapes of the PECs derived from v2RDM-CASSCF and v2RDM-CASSCF-PDFT, relative to that from CASPT2. However, tBLYP is the only method that displays an unphysical hump in the dissociation limit. The NPEs for v2RDM-CASSCF, tSVWN3, tPBE, and tBLYP are 55.5, 64.0, 24.5, and 23.7 mE_h , respectively, when using RDMs that satisfy the PQG conditions. As noted above, the NPE for v2RDM-CASSCF is in much better agreement with that from CI-based CASSCF (both are 57.7 mE_h) when the RDMs satisfy the T2 condition. Again, full translation universally lowers the energy obtained from v2RDM-CASSCF-PDFT, and the corresponding NPEs are insensitive to the N -representability of the underlying RDMs. The largest change observed in the NPE is an increase of 0.6 mE_h , in the case of ftSVWN3 and tPBE.

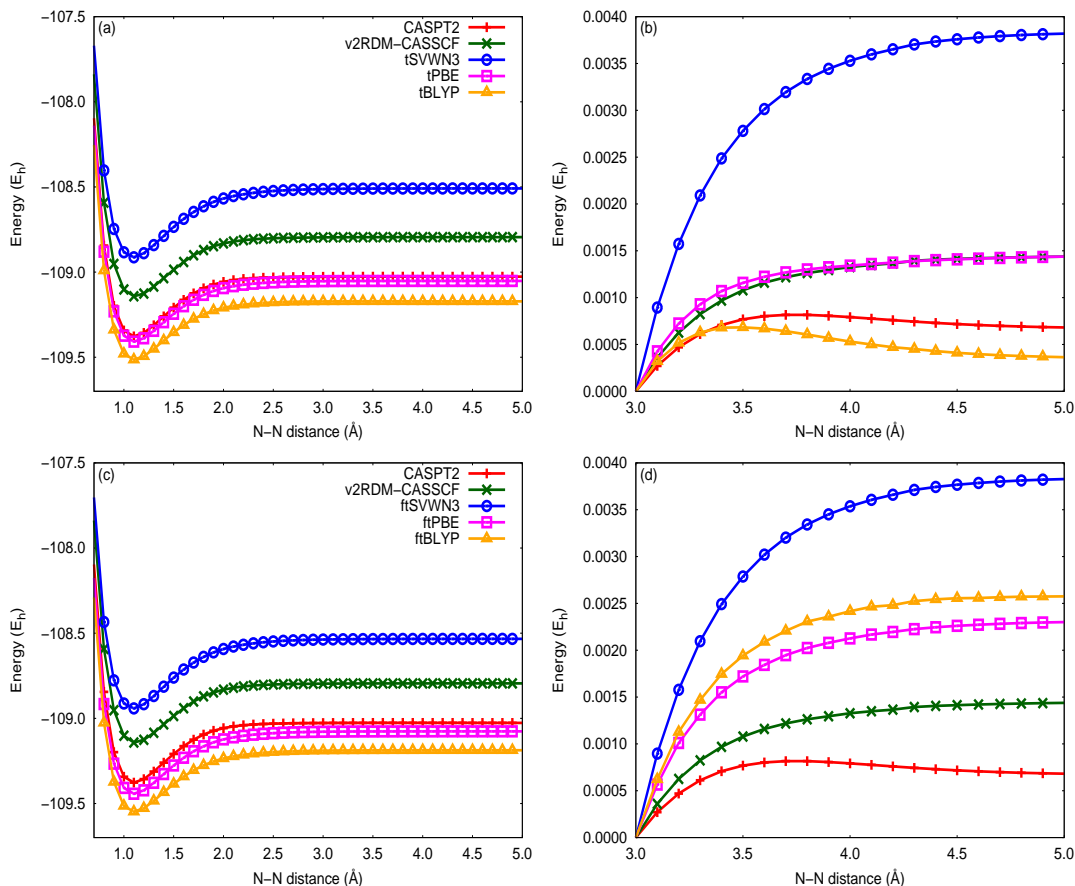
As an additional measure of the quality of the computed PECs, we consider the dissociation energy for N_2 and the double dissociation energy for H_2O . These values, along with estimates of the equilibrium bond lengths in these molecules, are presented in Table II; errors in computed dissociation energies are provided in parentheses. Here, an approximation to the dissociation energy is defined as the difference between energy computed at the equilibrium geometry and at stretched geometries with N–N or O–H bond lengths of 5.0 Å (the H–O–H angle of H_2O was fixed at 104.5°). The equilibrium bond lengths were estimated by fitting a quadratic function to each PECs around equilibrium and identifying the minimum in that function. The worst estimates of the dissociation energy are provided by v2RDM-CASSCF and either translated or fully-translated SVWN PDFT functionals, regardless of the N -representability conditions imposed in the reference v2RDM-CASSCF computations. Significantly improved results are obtained from the tPBE, ftPBE, and ftBLYP functionals; for both molecules, these functionals yield dissociation energies that are accurate to a few $kcal\ mol^{-1}$. The performance of the tBLYP functional is much worse for N_2 than it is for H_2O , which is a consequence of the unphysical hump in the tPBE PEC for N_2 that was discussed above. As with the NPE, dissociation energies from v2RDM-CASSCF-PDFT are less sensitive than those from v2RDM-CASSCF to the N -representability of the RDMs. For N_2 , the v2RDM-CASSCF dissociation energies change by approximately 6 $kcal\ mol^{-1}$ depending on whether or not the T2 condition is enforced; on the other hand, the corresponding v2RDM-CASSCF-PDFT dissociation energies differ by roughly 2 $kcal\ mol^{-1}$. For H_2O , the v2RDM-CASSCF double dissociation energy changes by about 1 $kcal\ mol^{-1}$ when enforcing the T2 condition, while the corresponding v2RDM-CASSCF-PDFT values change by only 0.1–0.2 $kcal\ mol^{-1}$.

TABLE I: Non-parallelity errors (mE_h) in the potential energy curves relative to curves generated at the CASPT2 level of theory.

Molecule ^a	N -representability	v2RDM-CASSCF	tSVWN3	tPBE	tBLYP	ftSVWN3	ftPBE	ftBLYP
N ₂	PQG	35.5	91.8	17.7	20.9	99.6	29.7	33.0
H ₂ O		55.5	64.0	24.5	23.7	66.4	27.2	28.6
CN ⁻		65.9	56.5	33.1	46.3	64.5	24.8	31.6
N ₂	PQG+T2	29.5	92.6	18.3	18.2	100.8	30.1	33.5
H ₂ O		57.7	64.4	25.1	23.2	67.0	27.2	28.5
CN ⁻		68.0	63.6	31.3	43.8	71.8	23.4	29.6

^a NPEs were evaluated for N–N, C–N, and O–O bond lengths in the ranges 0.7–5.0 Å, 0.7–5.0 Å, and 0.6–5.0 Å, respectively.

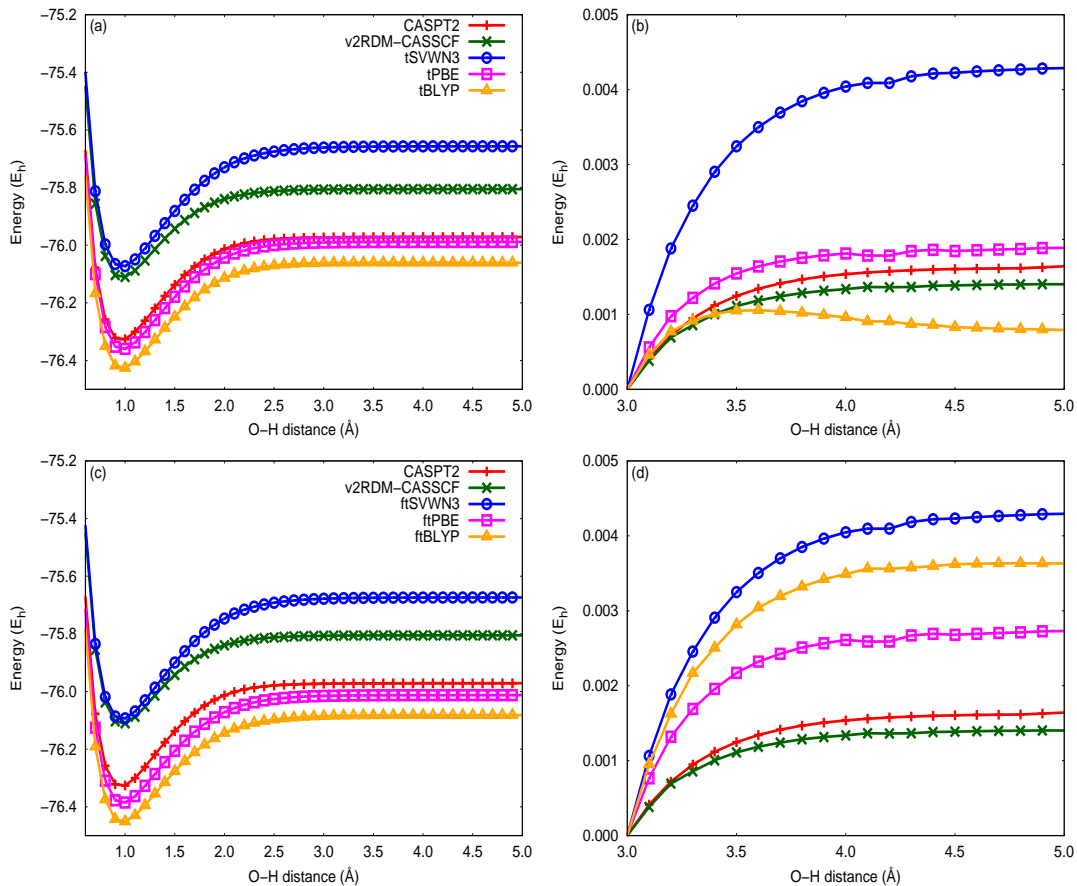
FIG. 1: Potential energy curves for the dissociation of N₂ within the cc-pVTZ basis set [(a), (c)], as well as their behavior in the limit of dissociation [(b), (d)]. RDMs from v2RDM-CASSCF employed within v2RDM-CASSCF-PDFT satisfy the PQG N -representability conditions. Results are provided using both the translated [(a), (b)] and fully-translated [(c), (d)] v2RDM-CASSCF-PDFT schemes.



The last PECs considered are those for the dissociation of CN⁻ in the cc-pVTZ basis set, which are depicted in Fig. 3. Some of the qualitative features of the v2RDM-CASSCF and v2RDM-CASSCF-PDFT derived PECs follow the same trends observed for N₂ and H₂O; for example, fully-translated functionals yield lower energies than translated ones, and tPBE and ftPBE are the most accurate flavors of v2RDM-CASSCF-PDFT, as measured by the absolute deviations from CASPT2. On the other hand, one notable difference stands out in this case: all v2RDM-based methods be-

have qualitatively incorrectly in the dissociation limit. It is well known that v2RDM-based approaches dissociate heteronuclear diatomic molecules into fractionally charged species; [99] the description of CN⁻ with v2RDM-CASSCF is one such case. This issue stems from a lack of derivative discontinuity in the energy as a function of electron number in isolated atoms, which has long been known to impact the quality of the description of the dissociation limit. [100] It is not surprising that v2RDM-CASSCF-PDFT built upon reference RDMs from v2RDM-CASSCF would display the same

FIG. 2: Potential energy curves for the symmetric dissociation of H₂O within the cc-pVTZ basis set [(a), (c)], as well as their behavior in the limit of dissociation [(b), (d)]. RDMs from v2RDM-CASSCF employed within v2RDM-CASSCF-PDFT satisfy the PQG N -representability conditions. Results are provided using both the translated [(a), (b)] and fully-translated [(c), (d)] v2RDM-CASSCF-PDFT schemes.



incorrect behavior. We also note that enforcing partial three-particle N -representability does not improve the situation; additional dissociation curves that demonstrate this failure can be found in the Supporting Information.

B. Singlet/Triplet Energy Gaps in Polyacene Molecules

The electronic structure of the linear polyacene series has long been of interest to experimentalists and theoreticians alike. The optical properties of these molecules, particularly their propensity to undergo singlet fission,[101–105] make them desirable components in photovoltaic devices.[106–111] The instability of the longer members of the series usually limits practical devices to those containing four or five fused benzene rings, but synthesis of polyacenes with up to nine fused benzene rings has been reported.[112–119]

The fascinating electronic structure of the larger members of the polyacene series has fueled a series of contentious interpretations of the results of state-of-the-art

electronic structure computations. These controversies began with debates over the ground spin state of the longer members of the series[120–125] and have evolved into a discussion over the degree to which the lowest-energy singlet state can be considered a closed-shell di- or polyradical.[58, 121, 123, 126–134] The former question has been settled; it is generally agreed upon that the singlet state is lower in energy than the triplet state for all linear acene molecules. Only recently, however, has it become clear that even methods capable of describing non-dynamical correlation effects in large active spaces (e.g. DMRG- or v2RDM-based CASSCF) tend to overestimate the polyradical character of the larger members of the series when correlations among the σ/σ^* network are ignored.[131–134] A detailed history of the progression of these controversies is recounted in Ref. 134.

In this Section, we explore the utility of v2RDM-CASSCF-PDFT for modeling the singlet/triplet energy gap in linear acene molecules. The literature is cluttered with estimates of this quantity generated using a variety of MR methods, including v2RDM-, [58, 129, 135] DMRG-, [55, 126, 128] adaptive CI (ACI)-, [130, 136] and MC-PDFT-based[55, 56] approaches, as

TABLE II: Equilibrium bond lengths (R , Å) and dissociation energies (D_e , kcal mol⁻¹) obtained from experiment, as well as from v2RDM-CASSCF and various PDFT functionals within the cc-pVTZ basis. Errors in computed dissociation energies are provided in parentheses.

Method	N -representability	N ₂		H ₂ O	
		R	D_e	R	D_e
v2RDM-CASSCF		1.12	217.8 (-10.7)	0.972	192.5 (-39.7)
tSVWN3		1.11	253.6 (25.1)	0.973	262.2 (30.0)
tPBE		1.11	223.5 (-5.1)	0.975	233.9 (1.7)
tBLYP	PQG	1.11	214.4 (-14.1)	0.976	230.2 (-2.0)
ftSVWN3		1.10	256.0 (27.5)	0.971	264.5 (32.3)
ftPBE		1.11	229.7 (1.1)	0.976	234.9 (2.7)
ftBLYP		1.11	226.0 (-2.5)	0.978	232.6 (0.4)
v2RDM-CASSCF		1.12	212.0 (-16.5)	0.971	191.5 (-40.7)
tSVWN3		1.11	255.9 (27.4)	0.974	262.2 (30.1)
tPBE		1.11	225.5 (-3.0)	0.976	233.8 (1.6)
tBLYP	PQG+T2	1.11	216.6 (-11.9)	0.977	230.1 (-2.1)
ftSVWN3		1.10	258.5 (29.9)	0.972	264.6 (32.4)
ftPBE		1.11	231.2 (2.7)	0.976	234.7 (2.5)
ftBLYP		1.11	227.8 (-0.7)	0.978	232.4 (0.3)
Experiment		1.098 ^{a,c}	227.8 ^{a,c}	0.958 ^{b,c}	232.2 ^d

^a From Refs. 93 and 94

^b From Refs. 95 and 96

^c From Ref. 97

^d From Ref. 98

well as with multireference-averaged quadratic coupled-cluster (MR-AQCC)[137, 138] and quantum Monte-Carlo methods.[134]. Nevertheless, no one approach has emerged as a panacea for this particular problem, for a variety of reasons. First, as mentioned above, nondynamical correlation effects are quite important for large members of the series, and, yet, even active spaces comprised of the full π/π^* valence space fail to correctly describe the onset of closed-shell diradical behavior. A proper description of these systems requires that one at least consider dynamical correlation effects, if not additional nondynamical correlation effects among the remaining valence orbitals. Second, most studies employ inconsistent levels of theory to evaluate the equilibrium molecular geometries and the singlet/triplet energy gaps; equilibrium geometries are usually determined using restricted or unrestricted DFT and the B3LYP functional. Such a choice often results in singlet/triplet energy gap curves that are not completely smooth.[56, 58, 134]

Figure 4 illustrates the singlet/triplet energy gap for the linear polyacene series computed using a variety of methods, including v2RDM-CASSCF and v2RDM-CASSCF-PDFT (labeled tPBE and tBLYP). All v2RDM-based computations employed an active space comprised of the π/π^* valence space ($4k+2$ electrons in $4k+2$ orbitals, where k is the number of fused benzene rings in the molecule). The v2RDM-based energy gaps presented here were computed within the cc-pVTZ basis set using equilibrium geometries optimized for the singlet and triplet states at the v2RDM-CASSCF/cc-pVDZ level of theory. We thus have some guarantee that the equilibrium geometries reflect the presence of nondynamical correlation effects, but we note that the structures dis-

play signatures of the overestimation of polyradical character mentioned above (see Refs. 134 and 91 for a discussion of these effects). Nonetheless, the v2RDM-CASSCF energy gaps agree well with those from DMRG[126], despite the fact that the DMRG data were generated using a smaller basis set and B3LYP-derived geometries. As expected, the dynamical correlation effects captured by v2RDM-CASSCF-PDFT close the singlet/triplet energy gap considerably for larger molecules, and we note that the tPBE and tBLYP functionals yield essentially equivalent gaps for all molecules. Surprisingly, DMRG-PDFT and v2RDM-CASSCF-PDFT give quite different results for hexacene and heptacene. The DMRG-PDFT data of Ref. 55 were generated within the 6-31+G(d,p) basis set, using B3LYP-derived geometries, but, these differences are still unanticipated, considering the good agreement we observe between the DMRG results of Ref. 126 and the present v2RDM-CASSCF results.

Figure 4 also includes data generated using a combined ACI / second-order perturbative multireference driven similarity renormalization group (DSRG-MRPT2) approach and the particle-particle random phase approximation (pp-RPA), taken from Refs. 136 and 139, respectively. Of all methods considered here, ACI-DSRG-MRPT2 yields the best agreement with experimental results, up to pentacene. Assuming that ACI and DSRG-MRPT2 can be extended to larger members of this series, ACI-DSRG-MRPT2 appears to be an extremely promising approach for this problem. Direct comparisons to pp-RPA results are complicated by the fact that these gaps are vertical, whereas the present results and all others reproduced here are adiabatic. The label pp-RPA-R (pp-RPA-T) refers to computations performed at

FIG. 3: Potential energy curves for the dissociation of CN^- within the cc-pVTZ basis set [(a), (c)], as well as their behavior in the limit of dissociation [(b), (d)]. RDMs from v2RDM-CASSCF employed within v2RDM-CASSCF-PDFT satisfy the PQG N -representability conditions. Results are provided using both the translated [(a), (b)] and fully-translated [(c), (d)] v2RDM-CASSCF-PDFT schemes.

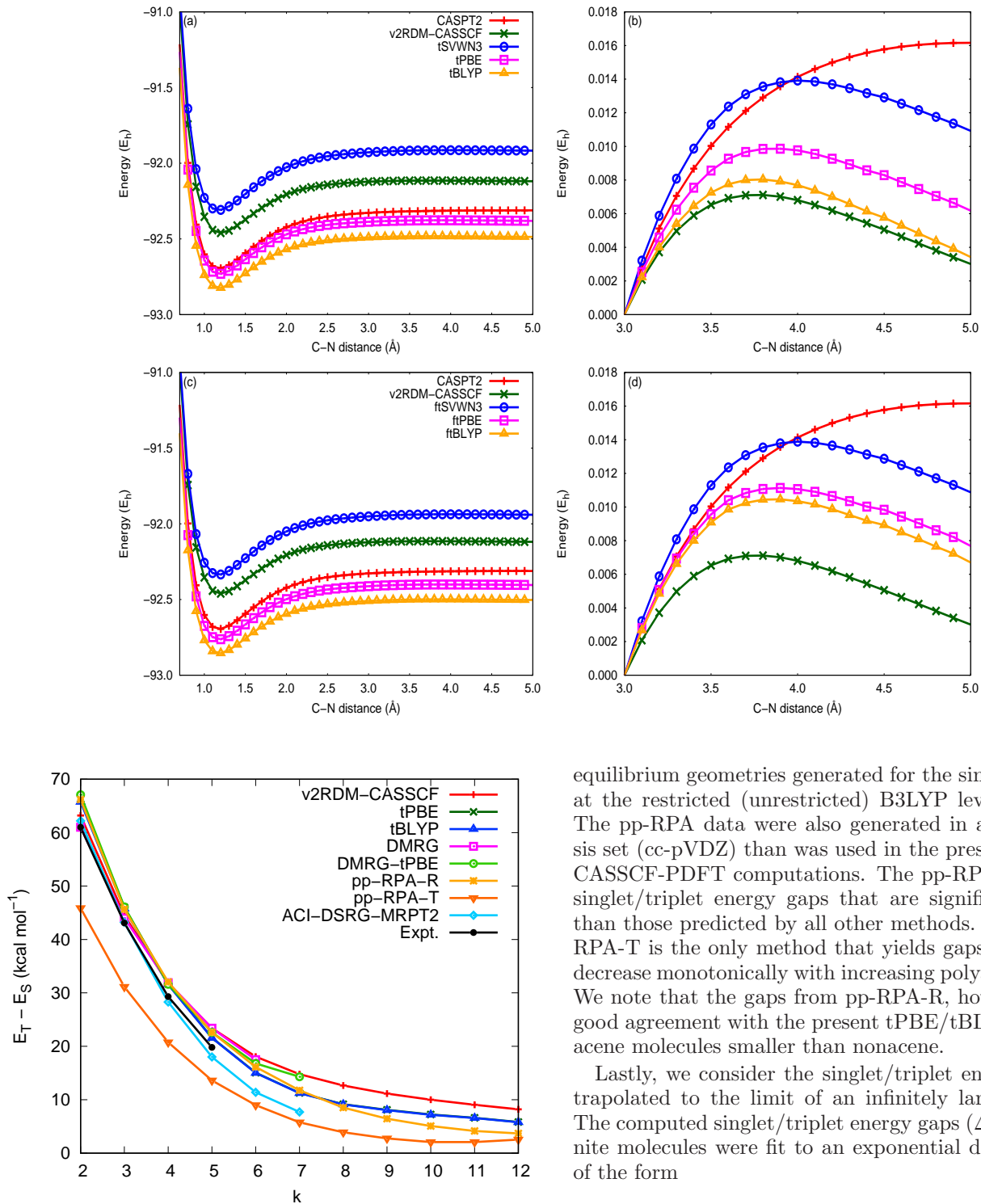


FIG. 4: Singlet-triplet energy gaps of the linear polyacene series. The label “ k ” refers to the number of fused benzene rings in each molecule.

equilibrium geometries generated for the singlet (triplet) at the restricted (unrestricted) B3LYP level of theory. The pp-RPA data were also generated in a smaller basis set (cc-pVDZ) than was used in the present v2RDM-CASSCF-PDFT computations. The pp-RPA-T predicts singlet/triplet energy gaps that are significantly lower than those predicted by all other methods. Further, pp-RPA-T is the only method that yields gaps that do not decrease monotonically with increasing polyacene length. We note that the gaps from pp-RPA-R, however, are in good agreement with the present tPBE/tBLYP gaps, for acene molecules smaller than nonacene.

Lastly, we consider the singlet/triplet energy gap extrapolated to the limit of an infinitely large molecule. The computed singlet/triplet energy gaps (ΔE_{S-T}) for finite molecules were fit to an exponential decay formula of the form

$$\Delta E_{S-T}(k) = ae^{-k/b} + c \quad (20)$$

where, a , b and c are adjustable parameters, and k represents the number of fused benzene rings in the molecule. In the limit that k approaches infinity, $c \sim \Delta E_{S-T}(\infty)$.

Table III summarizes the fitting parameters and predictions for $\Delta E_{S-T}(\infty)$ for the subset of methods considered above for which data are available up to $k = 12$. The largest predicted gap is obtained by v2RDM-CASSCF, which indicates that the limited considerations of non-dynamical correlation, combined with a lack of dynamical correlation, artificially stabilize the singlet state. The gaps predicted by tPBE and tBLYP are 4.87 and 4.79 kcal mol⁻¹, respectively. These values are in good agreement with the “best estimate” value of 5.06 kcal mol⁻¹ of Ref. 125, which was computed using a combination of spin-flip coupled-cluster and spin-flip time-dependent DFT. The smallest estimates for the infinite-acene singlet/triplet gap are given by pp-RPA-R and pp-RPA-T.

TABLE III: Fitting formulas for singlet-triplet energy gaps of polyacenes as a function of number of fused benzene rings k where $k \in [2, 12]$

Level of Theory	Fitting Formula
v2RDM-CASSCF/cc-pVTZ ^a	$127.79 \exp(-k/2.39) + 7.85$
tPBE/cc-pVTZ ^a	$147.15 \exp(-k/2.32) + 4.87$
tBLYP/cc-pVTZ ^a	$145.04 \exp(-k/2.33) + 4.79$
pp-RPA-R/cc-pVDZ ^b	$137.04 \exp(-k/2.63) + 2.11$
pp-RPA-T/cc-pVDZ ^b	$105.87 \exp(-k/2.37) + 0.81$

^a Geometries are optimized at v2RDM-CASSCF/cc-pVDZ level of theory.

^b Geometries are optimized at B3LYP/6-31G(d) level of theory.

V. CONCLUSIONS

Multiconfigurational pair-density functional theory provides a conceptually and technically straightforward framework within which one can combine the reliable description of nondynamical correlation effects afforded by multireference methods with the simplicity of DFT for modeling dynamical correlation. In practice, the computational cost of MC-PDFT is dominated entirely by the effort required to generate the 1- and 2-RDM using the underlying MR approach. Hence, polynomially-scaling approaches to the nondynamical correlation problem (e.g. v2RDM-CASSCF, DMRG-CASSCF[55], or pair coupled-cluster doubles[32]) are naturally suited to this purpose. Accordingly, we have presented an implementation of v2RDM-CASSCF-PDFT and benchmarked its performance on challenging MR problems.

We applied v2RDM-CASSCF-PDFT with the translated and fully-translated variants of the PBE, BLYP, and SVWN3 functionals to the dissociation of N₂ and CN⁻ and to the double dissociation of H₂O. In general, the best absolute agreement with potential energy curves generated at the CASPT2 level of theory was obtained using tPBE. It is notable that the quality of the v2RDM-CASSCF-PDFT curves, as measured by the non-parallelity error relative to CASPT2, was somewhat insensitive to the N -representability of the underlying

2-RDM. A similar insensitivity was observed in the dissociation energy for N₂ and the double dissociation energy for H₂O computed using v2RDM-CASSCF-PDFT. These results are potentially important because the cost of imposing three-particle N -representability conditions can be prohibitive for large systems. It seems that additional N -representability conditions may be necessary insofar as they improve the quality of the 1-RDM and on-top pair-density entering the v2RDM-CASSCF-PDFT energy expression. Further, we should note that even an exact treatment of the N -representability problem will not actually guarantee any improvement in the v2RDM-CASSCF-PDFT energy. Indeed, Sharma *et al.* have shown[140] for H₂ that the MC-PDFT energy does not converge to the exact (full CI) result even when the exact on-top pair-density is available. Regardless, additional studies are necessary to fully explore the role of N -representability in generating accurate densities and on-top pair densities and to determine whether the trends we have observed are transferable to other systems.

We also applied the tPBE and tBLYP functionals to the singlet/triplet energy gap of the linear polyacene series; these functionals predict the gap in the limit of an infinitely long acene molecule to be 4.87 and 4.79 kcal mol⁻¹, respectively. We note that a similar study has been carried out using MC-PDFT where the 1- and 2-RDM were generated using the generalized active space self-consistent field (GASSCF) method.[56] However, direct comparisons to the data presented in Ref. 56 are difficult because the GASSCF and GASSCF-PDFT results are sensitive to the partitioning chosen for the active space. For example, one choice leads to the prediction that the GASSCF-PDFT-derived singlet/triplet gap in the large molecule limit closes, relative to that from GASSCF, while another choice leads to the prediction that it opens. Further, regardless of how the active space was partitioned in that work, GASSCF-PDFT failed to yield a smooth singlet/triplet energy gap curve.

Lastly, we note a practical similarity between MC-PDFT and the density corrected DFT described by Burke and coworkers.[141–143] The latter approach addresses so-called “density-driven” errors by evaluating the exchange-correlation energy with an “accurate” density that differs from the self-consistent density one would normally obtain with a given functional. MC-PDFT can be viewed as a generalization of density-corrected DFT where the density used to evaluate the exchange correlation energy is obtained by translation[52] of the density generated by an MR method. As demonstrated in Ref. 32, the MR method need not be CASSCF-based; it could be any method that produces a good 1-RDM and on-top pair density. The v2RDM-CASSCF-PDFT PECs for CN⁻ highlight the fact that the approach is only as reliable as the densities generated by the MR method.

VI. APPENDIX

The fully-translated densities and gradients entering the fully-translated OTPD functional (defined in Eq. 19) are given by [73]

$$\tilde{\rho}_\sigma(\mathbf{r}) = \begin{cases} \frac{\rho(\mathbf{r})}{2} (1 + c_\sigma \zeta_t(\mathbf{r})) & R(\mathbf{r}) < R_0 \\ \frac{\rho(\mathbf{r})}{2} (1 + c_\sigma \zeta_{ft}(\mathbf{r})) & R_0 \leq R(\mathbf{r}) \leq R_1 \\ \frac{\rho(\mathbf{r})}{2} & R(\mathbf{r}) > R_1 \end{cases} \quad (21)$$

and

$$\nabla \tilde{\rho}_\sigma(\mathbf{r}) = \begin{cases} \frac{\nabla \rho(\mathbf{r})}{2} (1 + c_\sigma \zeta_t(\mathbf{r})) + c_\sigma \frac{\rho(\mathbf{r})}{2} \nabla \zeta_t(\mathbf{r}) & R(\mathbf{r}) < R_0 \\ \frac{\nabla \rho(\mathbf{r})}{2} (1 + c_\sigma \zeta_{ft}(\mathbf{r})) + c_\sigma \frac{\rho(\mathbf{r})}{2} \nabla \zeta_{ft}(\mathbf{r}) & R_0 \leq R(\mathbf{r}) \leq R_1 \\ \frac{\nabla \rho(\mathbf{r})}{2} & R(\mathbf{r}) > R_1 \end{cases} \quad (22)$$

where $R_0 = 0.9$ and $R_1 = 1.15$. [72, 73] The fully-translated spin-polarization factor $\zeta_{ft}(\mathbf{r})$ is taken to be

$$\zeta_{ft} = A\Delta R^5(\mathbf{r}) + B\Delta R^4(\mathbf{r}) + C\Delta R^3(\mathbf{r}) \quad (23)$$

where, $\Delta R(\mathbf{r}) = R(\mathbf{r}) - R_1$ and [72, 73]

$$A = -475.60656009 \quad (24)$$

$$B = -379.47331922 \quad (25)$$

$$C = -85.38149682 \quad (26)$$

The gradients of the translated and fully-translated spin-polarization factors are [72, 73]

$$\nabla \zeta_t(\mathbf{r}) = -\frac{1}{2} \frac{\nabla R(\mathbf{r})}{\zeta_t(\mathbf{r})} \quad (27)$$

$$\nabla \zeta_{ft}(\mathbf{r}) = \nabla R(\mathbf{r}) [5A\Delta R^4(\mathbf{r}) + 4B\Delta R^3(\mathbf{r}) + 3C\Delta R^2(\mathbf{r})] \quad (28)$$

where the gradient of the on-top ratio is [72]

$$\nabla R(\mathbf{r}) = \frac{4\nabla \Pi(\mathbf{r})}{\rho^2(\mathbf{r})} - \frac{8\Pi(\mathbf{r})\nabla \rho(\mathbf{r})}{\rho^3(\mathbf{r})}. \quad (29)$$

Supporting information. Active space specifications, singlet/triplet energy gaps for non-conjugated main-group divalent radicals, potential energy curves for N_2 , CN^- and H_2O dissociation computed using v2RDM-CASSCF / v2RDM-CASSCF-PDFT and the PQG+T2 N -representability conditions, and singlet/triplet energy gaps for linear polyacene molecules computed using v2RDM-CASSCF / v2RDM-CASSCF-PDFT and RDMs that satisfy the PQG N -representability conditions.

Acknowledgments This material is based upon work supported by the Army Research Office Small Business Technology Transfer (STTR) program under Grant No. W911NF-16-C-0124.

-
- [1] W. Kutzelnigg, *Theory of Electron Correlation in: Explicitly correlated wave functions in Chemistry and Physics* (Springer Netherlands, 2003), pp. 3–90, Progress in Theoretical Chemistry and Physics.
- [2] W. Kutzelnigg, *Electron correlation and electron pair theories* (Springer, Berlin, Heidelberg, 1973), pp. 31–73.
- [3] C. Hättig, W. Klopper, A. Köhn, and D. P. Tew, *Chem. Rev.* **112**, 4 (2012).
- [4] B. O. Roos, R. Lindh, P. A. Malmqvist, V. Veryazov, and P.-O. Widmark, *Multiconfigurational quantum chemistry* (Wiley, 2016).
- [5] T. Helgaker, P. Jørgensen, and J. Olsen, *Molecular Electronic-Structure Theory* (John Wiley & Sons, Inc., New York, 2000).
- [6] A. Szabo and N. S. Ostlund, *Modern quantum chemistry : introduction to advanced electronic structure theory* (Dover Publications, 1996).
- [7] D. R. Yarkony, *Modern Electronic Structure Theory*, vol. 2 of *Advanced Series in Physical Chemistry* (World Scientific Publishing Company, 1995).
- [8] R. G. Parr and W. Yang, *Density-functional theory of atoms and molecules* (Oxford University Press, 1989).
- [9] C. Fiolhais, F. Nogueira, and M. A. L. Marques, eds., *A Primer in Density Functional Theory*, vol. 620 of *Lecture Notes in Physics* (Springer Berlin Heidelberg, Berlin, Heidelberg, 2003).
- [10] A. J. Garza, G. E. Scuseria, A. Ruzsinszky, J. Sun, and J. P. Perdew, *Mol. Phys.* **114**, 928 (2016).
- [11] A. J. Cohen, P. Mori-Sánchez, and W. Yang, *Chem. Rev.* **112**, 289 (2012).
- [12] A. D. Becke, *J. Chem. Phys.* **140** (2014).
- [13] J. Cioslowski, ed., *Many-Electron Densities and Reduced Density Matrices*, Mathematical and Computational Chemistry (Springer US, Boston, MA, 2000).
- [14] E. R. Davidson, *Reduced density matrices in quantum chemistry* (Academic Press, 1976).
- [15] A. J. Coleman and V. I. Yukalov, *Reduced density matrices : Coulson's challenge* (Springer, 2000).
- [16] D. A. Mazziotti, *Reduced-density-matrix mechanics : with applications to many-electron atoms and molecules* (Wiley, 2007).
- [17] N. I. Gidopoulos and S. Wilson, *The Fundamentals of Electron Density, Density Matrix and Density Functional Theory in Atoms, Molecules and the Solid State* (Springer Netherlands, 2003).
- [18] T. Helgaker, S. Coriani, P. Jørgensen, K. Kristensen, J. Olsen, and K. Ruud, *Chem. Rev.* **112**, 543 (2012).
- [19] P. G. Szalay, T. Müller, G. Gidofalvi, H. Lischka, and R. Shepard, *Chem. Rev.* **112**, 108 (2012).
- [20] B. O. Roos, P. R. Taylor, and P. E. M. Siegbahn, *Chem. Phys.* **48**, 157 (1980).
- [21] P. Siegbahn, A. Heiberg, B. Roos, and B. Levy, *Phys. Scripta* **21**, 323 (1980).

- [22] P. E. M. Siegbahn, J. Almlöf, A. Heiberg, and B. O. Roos, *J. Chem. Phys.* **74**, 2384 (1981).
- [23] B. O. Roos, *The Complete Active Space Self-Consistent Field Method and its Applications in Electronic Structure Calculations* (John Wiley & Sons, Inc., 1987), vol. 68, pp. 399–445.
- [24] K. Andersson, P. A. Malmqvist, B. O. Roos, A. J. Sadlej, and K. Wolinski, *J. Phys. Chem.* **94**, 5483 (1990).
- [25] K. Andersson, P. Å. Malmqvist, and B. O. Roos, *J. Chem. Phys.* **96**, 1218 (1992).
- [26] D. Mukherjee and W. Kutzelnigg, *J. Chem. Phys.* **114**, 2047 (2001).
- [27] W. Kutzelnigg and D. Mukherjee, *J. Chem. Phys.* **120**, 7350 (2004).
- [28] D. A. Mazziotti, *Phys. Rev. Lett.* **97**, 143002 (2006).
- [29] F. A. Evangelista, *J. Chem. Phys.* **141** (2014).
- [30] G. C. Lie and E. Clementi, *J. Chem. Phys.* **60**, 1275 (1974).
- [31] G. C. Lie and E. Clementi, *J. Chem. Phys.* **60**, 1288 (1974).
- [32] A. J. Garza, I. W. Bulik, T. M. Henderson, and G. E. Scuseria, *J. Chem. Phys.* **142** (2015).
- [33] A. J. Pérez-Jiménez and J. M. Pérez-Jordá, *Phys. Rev. A* **75**, 012503 (2007).
- [34] R. Colle and O. Salvetti, *Theor. Chim. Acta* **53**, 55 (1979).
- [35] F. Moscardó and E. San-Fabián, *Phys. Rev. A* **44**, 1549 (1991).
- [36] A. J. Garza, C. A. Jiménez-Hoyos, and G. E. Scuseria, *J. Chem. Phys.* **138**, 134102 (2013).
- [37] S. Pazziani, S. Moroni, P. Gori-Giorgi, and G. B. Bachelet, *Phys. Rev. B* **73**, 155111 (2006).
- [38] S. Gusarov, P. Malmqvist, R. Lindh, and B. O. Roos, *Theor. Chim. Acta* **112**, 84 (2004).
- [39] S. Gusarov, P.-Å. Malmqvist, and R. Lindh, *Mol. Phys.* **102**, 2207 (2004).
- [40] R. Takeda, S. Yamanaka, and K. Yamaguchi, *Chem. Phys. Lett.* **366**, 321 (2002).
- [41] H. Stoll, *Chem. Phys. Lett.* **376**, 141 (2003).
- [42] J. Gräfenstein and D. Cremer, *Chem. Phys. Lett.* **316**, 569 (2000).
- [43] J. Gräfenstein and D. Cremer, *Mol. Phys.* **103**, 279 (2005).
- [44] B. Miehlisch, H. Soll, and A. Savin, *Mol. Phys.* **91**, 527 (1997).
- [45] S. Grimme and M. Waletzke, *J. Chem. Phys.* **111**, 5645 (1999).
- [46] W. Wu and S. Shaik, *Chem. Phys. Lett.* **301**, 37 (1999).
- [47] R. Pollet, A. Savin, T. Leininger, and H. Stoll, *J. Chem. Phys.* **116**, 1250 (2002).
- [48] T. Leininger, H. Stoll, H.-J. Werner, and A. Savin, *Chem. Phys. Lett.* **275**, 151 (1997).
- [49] N. O. Malcolm and J. J. McDouall, *J. Phys. Chem.* **100**, 10131 (1996).
- [50] E. Kraka, *Chem. Phys.* **161**, 149 (1992).
- [51] L. Gagliardi, D. G. Truhlar, G. L. Manni, R. K. Carlson, C. E. Hoyer, and J. L. Bao, *Acc. Chem. Res.* **50**, 66 (2017).
- [52] G. Li Manni, R. K. Carlson, S. Luo, D. Ma, J. Olsen, D. G. Truhlar, and L. Gagliardi, *J. Chem. Theory Comput.* **10**, 3669 (2014).
- [53] P. A. Limacher, P. W. Ayers, P. A. Johnson, S. De Baerdemacker, D. Van Neck, and P. Bultinck, *J. Chem. Theory Comput.* **9**, 1394 (2013).
- [54] T. Stein, T. M. Henderson, and G. E. Scuseria, *J. Chem. Phys.* **140**, 214113 (2014).
- [55] P. Sharma, V. Bernales, S. Knecht, D. G. Truhlar, and L. Gagliardi, p. arXivID: 1808.06273 (2018).
- [56] S. Ghosh, C. J. Cramer, D. G. Truhlar, and L. Gagliardi, *Chem. Sci.* **8**, 2741 (2017).
- [57] G. Gidofalvi and D. A. Mazziotti, *J. Chem. Phys.* **129**, 134108 (2008).
- [58] J. Fosso-Tande, T.-S. Nguyen, G. Gidofalvi, and A. E. DePrince III, *J. Chem. Theory Comput.* **12**, 2260 (2016).
- [59] J. L. Bao, A. Sand, L. Gagliardi, and D. G. Truhlar, *J. Chem. Theory Comput.* **12**, 4274 (2016).
- [60] K. Husimi, *Proceedings of the Physico-Mathematical Society of Japan. 3rd Series* **22**, 264 (1940).
- [61] J. E. Mayer, *Phys. Rev.* **100**, 1579 (1955).
- [62] P.-O. Löwdin, *Phys. Rev.* **97**, 1474 (1955).
- [63] E. Pérez-Romero, L. M. Tel, and C. Valdemoro, *Int. J. Quantum Chem.* **61**, 55 (1997).
- [64] C. Garrod and J. K. Percus, *J. Math. Phys.* **5**, 1756 (1964).
- [65] Z. Zhao, B. J. Braams, M. Fukuda, M. L. Overton, and J. K. Percus, *J. Chem. Phys.* **120**, 2095 (2004).
- [66] R. M. Erdahl, *Int. J. Quantum Chem.* **13**, 697 (1978).
- [67] J. Povh, F. Rendl, and A. Wiegeler, *Computing* **78**, 277 (2006).
- [68] J. Malick, J. Povh, F. Rendl, and A. Wiegeler, *SIAM J. Optim.* **20**, 336 (2009).
- [69] D. A. Mazziotti, *Phys. Rev. Lett.* **106**, 83001 (2011).
- [70] J. P. Perdew, A. Savin, and K. Burke, *Phys. Rev. A* **51**, 4531 (1995).
- [71] A. D. Becke, A. Savin, and H. Stoll, *Theor. Chim. Acta* **91**, 147 (1995).
- [72] A. M. Sand, C. E. Hoyer, K. Sharkas, K. M. Kidder, R. Lindh, D. G. Truhlar, and L. Gagliardi, *J. Chem. Theory Comput.* **14**, 126 (2018).
- [73] R. K. Carlson, D. G. Truhlar, and L. Gagliardi, *J. Chem. Theory Comput.* **11**, 4077 (2015).
- [74] See https://github.com/edeprince3/v2rdm_casscf for v2RDM-CASSCF v0.8, a variational two-electron reduced-density-matrix-driven approach to complete active space self-consistent field theory (2018).
- [75] J. M. Turney, A. C. Simmonett, R. M. Parrish, E. G. Hohenstein, F. A. Evangelista, J. T. Fermann, B. J. Mintz, L. A. Burns, J. J. Wilke, M. L. Abrams, et al., *WIRES Comput. Mol. Sci.* **2**, 556 (2012).
- [76] R. Gáspár, *Acta Physica Academiae Scientiarum Hungaricae* **35**, 213 (1974).
- [77] J. C. Slater, *Phys. Rev.* **81**, 385 (1951).
- [78] S. H. Vosko, L. Wilk, and M. Nusair, *Can. J. Phys.* **58**, 1200 (1980).
- [79] J. P. Perdew, K. Burke, and M. Ernzerhof, *Phys. Rev. Lett.* **77**, 3865 (1996).
- [80] A. D. Becke, *Phys. Rev. A* **38**, 3098 (1988).
- [81] C. Lee, W. Yang, and R. G. Parr, *Phys. Rev. B* **37**, 785 (1988).
- [82] See <https://github.com/edeprince3/mcpdft> for MCPDFT, a multiconfigurational pair-density functional theory approach that employs reduced-density matrices generated by variational two-electron reduced-density matrix methods (2018).
- [83] F. Aquilante, J. Autschbach, R. K. Carlson, L. F. Chibotaru, M. G. Delcey, L. De Vico, I. Fdez. Galván,

- N. Ferré, L. M. Frutos, L. Gagliardi, et al., *J. Comput. Chem.* **37**, 506 (2016).
- [84] N. Forsberg and P.-Å. Malmqvist, *Chem. Phys. Lett.* **274**, 196 (1997).
- [85] G. Ghigo, B. O. Roos, and P. Å. Malmqvist, *Chem. Phys. Lett.* **396**, 142 (2004).
- [86] J. L. Whitten, *J. Chem. Phys.* **58**, 4496 (1973), arXiv:1011.1669v3.
- [87] B. I. Dunlap, J. W. D. Connolly, and J. R. Sabin, *J. Chem. Phys.* **71**, 3396 (1979).
- [88] T. H. Dunning, *J. Chem. Phys.* **90**, 1007 (1989).
- [89] F. Weigend, *Phys. Chem. Chem. Phys.* **4**, 4285 (2002).
- [90] Y. Shao, Z. Gan, E. Epifanovsky, A. T. Gilbert, M. Wormit, J. Kussmann, A. W. Lange, A. Behn, J. Deng, X. Feng, et al., **113**, 184 (2015), URL <https://doi.org/10.1080/00268976.2014.952696>.
- [91] J. W. Mullinax, E. Epifanovsky, G. Gidofalvi, and A. E. DePrince, *J. Chem. Theory Comput.* **0**, Just Accepted (0).
- [92] R. A. Kendall, T. H. Dunning, and R. J. Harrison, *J. Comp. Phys.* **96**, 6796 (1992).
- [93] K. P. Huber and G. Herzberg, *Molecular Spectra And Molecular Structure, IV. Constants Of Diatomic Molecules* (Van Nostrand Reinhold Co., Princeton, NJ, 1979).
- [94] W. C. Ermler, A. D. McLean, and R. S. Mulliken, *J. Phys. Chem.* **86**, 1305 (1982).
- [95] B. d. Darwent, *Nat. Stand. Ref. Data Ser.* **31** (????).
- [96] A. R. Hoy and P. R. Bunker, *J. Mol. Spectrosc.* **74**, 1 (1979).
- [97] *Computational chemistry comparison and benchmark database: National institute of standards and technology*, <https://cccbdb.nist.gov>.
- [98] S. Kurth, J. P. Perdew, and P. Blaha, *Int. J. Quantum Chem.* **75**, 889 (1999).
- [99] H. Van Aggelen, P. Bultinck, B. Verstichel, D. Van Neck, and P. W. Ayers, *Phys. Chem. Chem. Phys.* **11**, 5558 (2009).
- [100] J. P. Perdew, R. G. Parr, M. Levy, and J. L. Balduz, *Phys. Rev. Lett.* **49**, 1691 (1982).
- [101] M. J. Tayebjee, D. R. McCamey, and T. W. Schmidt, *J. Phys. Chem. Lett.* **6**, 2367 (2015).
- [102] M. C. Hanna and A. J. Nozik, *Journal of Applied Physics* **100**, 074510 (2006).
- [103] P. M. Zimmerman, F. Bell, D. Casanova, and M. Head-Gordon, *J. Am. Chem. Soc.* **133**, 19944 (2011).
- [104] M. W. B. Wilson, A. Rao, B. Ehrler, and R. H. Friend, *Acc. Chem. Res.* **46**, 1330 (2013).
- [105] S. Izadnia, D. W. Schönleber, A. Eisfeld, A. Ruf, A. C. LaForge, and F. Stienkemeier, *J. Phys. Chem. Lett.* **8**, 2068 (2017).
- [106] S. Yoo, B. Domercq, and B. Kippelen, *Appl. Phys. Lett.* **85**, 5427 (2004).
- [107] A. C. Mayer, M. T. Lloyd, D. J. Herman, T. G. Kasen, and G. G. Malliaras, *Appl. Phys. Lett.* **85**, 6272 (2004).
- [108] C.-W. Chu, Y. Shao, V. Shrotriya, and Y. Yang, *Appl. Phys. Lett.* **86**, 243506 (2005).
- [109] I. Paci, J. C. Johnson, X. Chen, G. Rana, D. Popović, D. E. David, A. J. Nozik, M. A. Ratner, and J. Michl, *J. Am. Chem. Soc.* **128**, 16546 (2006).
- [110] B. P. Rand, J. Genoe, P. Heremans, and J. Poortmans, *Prog. Photovolt. Res. Appl.* **15**, 659 (2007).
- [111] Y. Shao, S. Sista, C.-W. Chu, D. Sievers, and Y. Yang, *Appl. Phys. Lett.* **90**, 103501 (2007).
- [112] J. B. Birks, *Photophysics of aromatic molecules* (Wiley-Interscience, London, 1970).
- [113] J. Schiedt and R. Weinkauff, *Chem. Phys. Lett.* **266**, 201 (1997).
- [114] H. Angliker, E. Rommel, and J. Wirz, *Chem. Phys. Lett.* **87**, 208 (1982).
- [115] N. Sabbatini, M. T. Indelli, M. T. Gandolfi, and V. Balzani, *J. Phys. Chem.* **86**, 3585 (1982).
- [116] J. Burgos, M. Pope, C. E. Swenberg, and R. R. Alfano, *Phys. Status Solidi B* **83**, 249 (1977).
- [117] R. Mondal, C. Tönshoff, D. Khon, D. C. Neckers, and H. F. Bettinger, *J. Am. Chem. Soc.* **131**, 14281 (2009).
- [118] C. Tönshoff and H. Bettinger, *Angew. Chem. Int. Ed.* **49**, 4125 (2010).
- [119] S. Zade and M. Bendikov, *Angew. Chem. Int. Ed.* **49**, 4012 (2010).
- [120] K. N. Houk, P. S. Lee, and M. Nendel, *J. Org. Chem.* **66**, 5517 (2001).
- [121] M. Bendikov, H. M. Duong, K. Starkey, K. N. Houk, E. A. Carter, and F. Wudl, *J. Am. Chem. Soc.* **126**, 7416 (2004).
- [122] D.-e. Jiang and S. Dai, *J. Phys. Chem. A* **112**, 332 (2008).
- [123] B. Hajgató, D. Szieberth, P. Geerlings, F. De Proft, and M. S. Deleuze, *J. Chem. Phys.* **131**, 224321 (2009), ISSN 00219606.
- [124] C.-S. Wu and J.-D. Chai, *J. Chem. Theory Comput.* **11**, 2003–2011 (2015).
- [125] C. U. Ibeji and D. Ghosh, *Phys. Chem. Chem. Phys.* **17**, 9849 (2015).
- [126] J. Hachmann, J. J. Dorando, M. Avilés, and G. K.-L. Chan, *J. Chem. Phys.* **127**, 134309 (2007).
- [127] G. Gidofalvi and D. A. Mazziotti, *J. Chem. Phys.* **129**, 134108 (2008).
- [128] W. Mizukami, Y. Kurashige, and T. Yanai, *J. Chem. Theory Comput.* **9**, 401 (2013).
- [129] J. Fosso-Tande, D. R. Nascimento, and A. E. DePrince III, *Mol. Phys.* **114**, 423 (2016).
- [130] J. B. Schriber and F. A. Evangelista, *J. Chem. Phys.* **144**, 161106 (2016).
- [131] J. Lee, D. W. Small, E. Epifanovsky, and M. Head-Gordon, *J. Chem. Theory Comput.* **13**, 602 (2017).
- [132] S. Battaglia, N. Faginas-Lago, D. Andrae, S. Evangelisti, and T. Leininger, *J. Phys. Chem. A* **121**, 3746 (2017).
- [133] S. Lehtola, J. Parkhill, and M. Head-Gordon, *Mol. Phys.* **116**, 547 (2018).
- [134] N. Dupuy and M. Casula, *J. Chem. Phys.* **148**, 134112 (2018).
- [135] K. Pelzer, L. Greenman, G. Gidofalvi, and D. A. Mazziotti, *J. Phys. Chem. A* **115**, 5632 (2011).
- [136] J. B. Schriber, K. P. Hannon, and F. A. Evangelista, p. arXivID: 1808.09403 (2018).
- [137] F. Plasser, H. Pašalić, M. H. Gerzabek, F. Libisch, R. Reiter, J. Burgdörfer, T. Müller, R. Shepard, and H. Lischka, *Angew. Chem. Int. Ed.* **52**, 2581 (2013).
- [138] S. Horn, F. Plasser, T. Müller, F. Libisch, J. Burgdörfer, and H. Lischka, *Theor. Chem. Acc.* **133**, 1511 (2014).
- [139] Y. Yang, E. R. Davidson, and W. Yang, *Proc. Nat. Acad. Sci.* **113**, E5098 (2016).
- [140] P. Sharma, D. G. Truhlar, and L. Gagliardi, *J. Chem. Theory Comput.* **14**, 660 (2018).
- [141] M.-C. Kim, E. Sim, and K. Burke, *Phys. Rev. Lett.* **111**, 073003 (2013).

- [142] M.-C. Kim, E. Sim, and K. Burke, *J. Chem. Phys.* **140**, 18A528 (2014).
- [143] M.-C. Kim, H. Park, S. Son, E. Sim, and K. Burke, *J. Phys. Chem. Lett.* **6**, 3802 (2015).